

IPTC 11722-PP

## IMPROVED CHARACTERISATION AND MODELLING OF CARBONATE RESERVOIRS FOR PREDICTING WATERFLOOD PERFORMANCE

S.K. Masalmeh and X.D. Jing, Shell Technology Oman

Copyright 2007, International Petroleum Technology Conference

This paper was prepared for presentation at the International Petroleum Technology Conference held in Dubai, U.A.E., 4–6 December 2007.

This paper was selected for presentation by an IPTC Programme Committee following review of information contained in an abstract submitted by the author(s). Contents of the paper, as presented, have not been reviewed by the International Petroleum Technology Conference and are subject to correction by the author(s). The material, as presented, does not necessarily reflect any position of the International Petroleum Technology Conference, its officers, or members. Papers presented at IPTC are subject to publication review by Sponsor Society Committees of IPTC. Electronic reproduction, distribution, or storage of any part of this paper for commercial purposes without the written consent of the International Petroleum Technology Conference is prohibited. Permission to reproduce in print is restricted to an abstract of not more than 300 words; illustrations may not be copied. The abstract must contain conspicuous acknowledgment of where and by whom the paper was presented. Write Librarian, IPTC, P.O. Box 833836, Richardson, TX 75083-3836, U.S.A., fax 01-972-952-9435.

### Abstract

Carbonate reservoirs are highly heterogeneous and often show oil-wet or mixed-wet characteristics. Both geological heterogeneity and wettability have strong impact on capillary pressure ( $P_c$ ) and relative permeability ( $K_r$ ) behaviour, which is controlled by the pore size distribution, interfacial tension and interactions between rock and fluids as well as the saturation history. Capillary pressure data are essential input in both static and dynamic modelling of heterogeneous carbonate reservoirs. Drainage  $P_c$  is generally used for initialising reservoir static models while imbibition  $P_c$  is used to model secondary and tertiary recovery processes.

The objective of this paper is to present an improved reservoir characterisation and modelling procedure for predicting waterflood performance of a Cretaceous carbonate reservoir in the Middle East. We focus on the characterisation of multi-phase fluid flow properties, in particular the capillary pressure characteristics in both drainage and imbibition, and their assignments in reservoir simulation models. We show that for modelling initial saturation distribution in the reservoir, assigning saturation functions based on permeability or porosity classes alone is not adequate. Moreover the petrophysical correlations often used for clastic reservoirs (e.g., Leverett J-function) may not be applicable to carbonate reservoirs without careful pore-type examination and core analysis/calibration.

A novel procedure is described to derive imbibition capillary pressure curves from the primary drainage  $P_c$  curves taking into account of wettability and fluid trapping. The results lead to an improved understanding of capillary pressure characteristics in carbonate reservoirs, in particular, the contact angle distributions and hysteresis behaviour in both drainage and imbibition. This paper also presents a mathematical model for implementing both drainage and

imbibition capillary pressure functions in dynamic reservoir simulation. This model takes into account the complex pore size distribution and wettability characteristics in carbonates as observed in experimental special core analysis (SCAL) measurements. Furthermore, how to assign imbibition  $P_c$  for the different porosity and permeability classes will be examined and its impact on modelling waterflooding performance and remaining oil saturation distributions assessed.

### Introduction

The complexity of carbonate reservoirs and the importance of a consistent approach in defining rock types have been a subject of several recent papers (Marzouk et al. 2000; Ramakrishnam et al. 2000; Leal et al. 2001; Porrai and Campos 2001; Giot et al. 2000; Silva et al. 2002; Hamon 2002; Masalmeh and Jing 2004). Current practices in general are either based on petrophysical properties (i.e., porosity, permeability and drainage  $P_c$  curves) or geological description (facies and depositional environment) or a combination of both. The underlying assumption is that static rock characterisation and the resultant rock-typing scheme remain valid when assigning saturation functions ( $P_c$  &  $K_r$ ) in dynamic reservoir modelling. In this paper, we will incorporate conventional core analysis (porosity, permeability), thin section and SEM analysis, mercury-air capillary pressure ( $P_c$ )/ NMR with special core analysis data, in particular, the imbibition  $P_c$  and residual oil saturation.

Several experimental techniques are available to measure capillary pressure ( $P_c$ ) curves, both in drainage and imbibition cycles. Mercury injection is frequently used for measuring drainage  $P_c$  curves as the technique is relatively cheap, fast and requires relatively straightforward data interpretation. The measured data, however, need to be converted to in situ reservoir conditions by taking into account the differences in interfacial tension and contact angle between the rock/fluid systems used in the laboratory and that found in reservoir. The porous-plate equilibrium method is a reliable and accurate technique for measuring  $P_c$  in drainage and imbibition under representative reservoir conditions of fluids, pressure and temperature. The main drawback of this technique is the lengthy time required to reach capillary equilibrium, which renders the technique impractical for certain field applications especially for tight and heterogeneous carbonates. The multi-speed centrifuge method can be used for both drainage and imbibition  $P_c$  measurements using representative reservoir fluids. Compared with the porous-plate equilibrium technique,

the centrifuge method is relatively fast, which is a clear advantage for studying tight carbonates. However, the design of the centrifuge experiment and the interpretation of the data are not straightforward and numerical simulation of centrifuge experiments is generally required to derive capillary pressure data (Maas and Schulte 1997).

The impact of capillary forces on multiphase flow and hydrocarbon recovery has been studied extensively in the literature. However, the focus has often been on the drainage capillary pressure curves, which are used for reservoir rock classification or rock typing and the initialization of reservoir static models. Several authors have discussed the complexity of obtaining a consistent set of drainage capillary pressure curves from the different techniques available (Honarpour et al. 2004; Sallier and Hamon 2005; Masalmeh and Jing 2004 and 2006). Although the experimental procedures are well established, the results of measured drainage Pc curves based on different techniques are not always conclusive and conflicting data are often encountered (e.g., when comparing data from different fluid pairs for the same rock). One of the reasons for the discrepancies is due to the ineffective core cleaning (a particular challenge for carbonates) to establish consistent wettability conditions mimicking the primary drainage process in the reservoir.

The impact of imbibition capillary pressure on waterflood sweep efficiency for heterogeneous oil-wet carbonates has been demonstrated previously (Masalmeh et al. 2003 and 2007). The complete capillary pressure curves covering primary drainage, imbibition and secondary drainage cycles on a rock-type basis are required as input for modelling secondary and tertiary reservoir recovery options for heterogeneous carbonate reservoirs. The waterflood remaining oil distribution depends strongly on the imbibition capillary pressure contrasts between various rock types in heterogeneous carbonates.

It is beyond the scope of this paper to give any in-depth treatment of the geological and petrophysical aspects of carbonate reservoir characterization and permeability mapping. Interested readers are referred to previous publications in this important topic area (e.g., Lucia 1999; Jennings and Lucia 2003). Instead we will focus on the dynamic properties especially imbibition capillary pressure and fluid trapping characteristics and their links with static rock properties (porosity, permeability and drainage capillary pressure). Experimental measurements have been performed on carbonate samples from a Cretaceous heterogeneous Middle East reservoir to cover the following aspects:

1. Measurements and interpretation of capillary pressure curves in the primary drainage and imbibition cycles.
2. Comparison of drainage Pc curves measured using the two different methods (mercury injection vs. centrifuge) for different porosity and permeability ranges.
3. The impact of core cleaning on primary drainage and imbibition water-oil capillary pressure curves.
4. Relating imbibition capillary pressure with primary drainage for both uni-modal and bi-modal pore size

distributions taking into account the effect of wettability and fluid trapping.

5. The impact of dynamic reservoir characterisation on the prediction of waterflood performance and remaining oil distributions.

### Experimental Procedure and Data Interpretation

A comprehensive special core analysis (SCAL) program was carried out on core samples taken from this carbonate field. Figure 1 shows the plot of porosity vs. permeability of the sample set, indicating that the permeability varies by up to three orders of magnitude for a relatively narrow porosity range. This range of permeability variation is common for such kind of carbonate reservoirs, which presents a challenge in classifying carbonates into rock types for permeability modelling and the subsequent imbibition Pc and Kr characterisation. Figure 2 shows the porosity and permeability distributions against the normalized reservoir depth. Most of the STOIP is located in rock types with the porosity range between 20-30%.

A set of 160 samples were selected from different permeability and porosity ranges representing all predominant geological facies for the subsequent special core analysis programme (Masalmeh and Jing 2004). It includes thin section and SEM rock characterisation, CT scanning, NMR and Hg-air Pc, oil/water primary drainage capillary pressure measurements (for comparison with Hg-air derived Pc), aging the samples in crude oil at connate water under reservoir temperature to restore wettability, spontaneous imbibition measurements followed by the forced imbibition and secondary drainage centrifuge experiments.

**Thin sections and SEM analysis:** All the samples used in this study were prepared for thin section and SEM analysis. Each of the thin sections has a detailed petrographic description, concentrating on texture, composition, cements and diagenesis and pore type. In addition, diagenetic evolution, depositional environment and reservoir properties were outlined. The samples have been classified using Dunham (1962)'s textural classification for carbonate rocks. The analysed samples predominantly consist of grainstones and packstones. Porosity habit and abundance in these samples is strongly affected by texture. Grainstone fabrics are generally characterised by good to very good and well to fairly well connected interparticle pores, followed by subordinate sparse to very sparse, usually isolated intraparticle porosity. Oversized pores, as well as micro-fractures are also locally present, with a certain amount of microporosity within granular components. Packstones are characterised by the progressive disappearance (with depth) of interparticle porosity (ranging, in the uppermost samples, from good to sparse). The main porosity types of these lithologies consist of sparse to common mouldic porosity, coupled by sparse to rare intraparticle porosity.

**Mercury air drainage capillary pressure:** Drainage capillary pressure is used to initialise reservoir static model, i.e., to determine saturation as a function of height above free water level (FWL) in conjunction with saturation logs, and to

calculate stock tank oil initially in place (STOIP) or gas initially in place (GIIP) of hydrocarbon reservoirs. It is also used for deriving pore size distributions and classifying rock types.

The mercury/air capillary pressure curves and the derived pore-throat size distributions have been measured using core plugs of 15 mm in diameter and 22 mm long which have been drilled in the vicinity of the selected SCAL plugs. Since the mercury-air capillary pressure data is often used as a basis for rock typing in combination with porosity/permeability trends, a detailed study of the available Pc curves is performed to identify possible trends or correlations with different rock properties such as permeability and pore types. The primary drainage Pc curves and corresponding pore throat size distribution data of the predominant rock types are shown in Figures 3-4. The following observations can be made:

1. The samples can be divided into three groups based on the shape of the capillary pressure curves.
  - a. Group A is mainly of bi-modal nature, it has a low entry pressure and at certain saturation the capillary pressure starts to increase. The permeability of this group varies between 40-1000 md and porosity between 27-31%.
  - b. Group B is characterised by a uni-model pore size distribution showing a capillary entry pressure of 1-3 psi and a gradual capillary pressure increase as saturation decreases indicating a wide range of pore size distribution hence a relatively large transition zone. The permeability of this group of samples varies between 10-40 md and the porosity ranges between 20-30%.
  - c. Group C has an entry pressure of more than 5 psi and a clear Pc plateau indicating a rather uniform pore size distribution. The permeability of the samples in this group varies between 0.5-10 md and porosity between 16-30%.
2. No clear correlation can be found between capillary pressure and the Dunham geological rock classifications. For example, grainstone samples in general have different capillary pressure, and some samples from different rock classes may have very similar drainage capillary pressure characteristics.
3. There is a clear correlation between permeability and entry pressure, the lower the permeability the higher the entry pressure and vice versa. For bi-modal pore systems, the capillary entry pressures are low and permeabilities are relatively high.
4. Within each Pc group described above there is a weak correlation between connate water and porosity, i.e., connate water saturation increases as porosity decreases. However, across Pc groups there is no clear correlation between connate water saturation and porosity. Low porosity samples from group C may have lower connate water than higher porosity sample from group A or B.
5. There is no correlation between connate water

saturation and permeability. Some low permeable samples show lower connate water saturation than the high permeability samples. This is due to the fact that the permeability is dominated by the large pore size population whereas connate water is controlled by the relative small pore size population, and there seems to be no correlation between the large and small pore populations due to the geological origin and complex diagenetic effects. This shows that any attempt to correlate connate water saturation with permeability, as often carried in sandstone reservoirs, will be fruitless here due to the complex pore systems in this carbonate reservoir.

**Leverett-J function:** Since usually only a limited number of capillary pressure curves are available, different models have been developed to relate capillary pressure curves with porosity and permeability, and to generate saturation vs. height functions (e.g., Harrison and Jing 2001). The Leverett J-function is one of the most commonly used formulations.

The J-function was originally proposed to convert all capillary pressure data for clean sands to a universal curve. However, attempts have also been made to use the J-function for carbonates. The data measured on the reservoir core under study is used to check the applicability of the J-function. Figure 5 shows the J-functions of group B samples ( $10 < K < 40$  md) corresponding to the drainage Pc curves of Figure 3.B. The Pc curves show that the samples can be divided into two sub-groups, whereas the J-function curves are separated into more than two groups. Converting the Pc curves of group A into J-function curves generates four distinct groups with quite different J-functions. For samples from group C, where the J-function curves collapse to almost one curve at connate water but show increased separation at the entry pressures. This shows that for carbonates (especially the highly heterogeneous dual porosity systems) the use of a general J-function is prone to errors, and the J-function should only be used with sufficient core data support and careful sub-zonation when initialising the static model.

**Nuclear Magnetic Resonance (NMR) T2 measurements:** The NMR T2 measurements provide another means for characterising the pore (body) size distributions. NMR T2 relaxation spectrum measurements have been performed on the plug samples at 100% water saturation. Similar to the pore throat size distribution obtained from Hg-air measurements, NMR data shows three distinct groups. Group A exhibits a dual-porosity behaviour, group B shows a wide pore size distribution and group C shows a narrow pore size distribution. One sample from each group is shown in Figure 6 for illustration purpose. Combining the results of the NMR and Hg-air measurements shows some important features such as the general average pore throat to pore body size ratios. For example, some samples show smaller pore throat sizes and yet larger pore body sizes. However the interpretation of NMR T2 distribution in carbonates and relating it to pore (body) size distribution is not quite straightforward. Some assumptions such as the fast diffusion regime and uniform surface relaxivity are often made in a general approach. Detailed pore

network modelling of NMR responses is recommended to take into account the full physics and relate NMR relaxation time distributions to corresponding pore (body) size distributions (e.g., Moctezuma et al. 2003; Valvatne et al. 2004).

### Mercury Injection vs. Centrifuge Capillary Pressure Curves

It is common practice to use Hg-air derived Pc curves to initialise static reservoir models and calculate oil in place. The Hg-air Pc curves can be converted to oil-water drainage Pc curves using the following equation:

$$P_{C_R} = P_{C_L} \frac{\sigma_R \cos(\theta)_R}{\sigma_L \cos(\theta)_L} \quad (1)$$

where  $\sigma$  is the interfacial tension (IFT) between the two fluids,  $\theta$  is the contact angle, subscript L refers to laboratory (Hg-air) and R refers to reservoir (oil-water) fluids. For detailed review and discussion on relating mercury injection data to equivalent oil-water systems, see Morrow and Melrose (1991) and the references therein.

In the centrifuge experiment, the average saturation in a core plug is recorded at a set of centrifugal speeds and then a capillary pressure vs. saturation point is calculated at each speed. The capillary pressure can be calculated from the centrifuge raw data using either analytical (e.g. Hassler-Brunner 1945; Forbes 1997) or numerical interpretation (Maas and Schulte 1997). The experimental data gathered for this study have been interpreted by numerical simulation using MoReS, the Shell in-house simulator, and compared against the conventional analytical techniques.

There are several factors that can affect the Hg-air and oil-water centrifuge drainage Pc curves and result in discrepancies. First, the interaction of rock and fluids (e.g., the existence of swelling clays) may cause the air/brine or oil/brine Pc curve to differ from the air/Hg derived Pc curves but this is generally not applicable to carbonates. Second, since the two measurements use different fluid systems, the contact angle (i.e., wettability) and its hysteresis may show different behaviours during the Pc experiments which, if not taken into account properly, may also complicate the conversion from mercury injection to oil-brine Pc measurements. Third, while the mercury-air experiment mimics strongly water-wet conditions, the water-oil experiment is affected by wettability in case the sample was not thoroughly cleaned, (O'Meara et al. 1992; Masalmeh and Jing 2004 and 2006; Sallier and Hamon 2005). If the sample is not properly cleaned then the contact angle in the oil-water primary drainage can be significantly larger than zero and  $\cos(\theta)$  can be significantly less than 1. Finally, since the two Pc measurements (Hg-air and oil-brine) are generally not performed on the same samples, geological heterogeneity may also cause discrepancy. In general the mercury injection experiment is either performed on the end trims of the plugs used in the water-oil experiments or, as in the case of this study, the mercury injection is performed on small samples

drilled next to the SCAL plugs.

We observed previously (Masalmeh and Jing 2004, 2006) that the capillary pressures measured using centrifuge and mercury injection methods showed a close match for some samples but there was a clear discrepancy for other samples. For those samples that did not show agreement the centrifuge oil-brine capillary pressure was always lower than the Hg-air derived Pc, i.e., at the same wetting phase saturation a lower capillary pressure was obtained in the oil-water system than in the Hg-air system after conversion with equation (1). In order to further investigate this, more SCAL data have been obtained and a thorough comparison has been made between Hg-air and water-oil centrifuge capillary pressure curves on about 50 samples from different porosity and permeability classes of the carbonate reservoir. Moreover, water-air drainage Pc curves have also been measured on a number of samples and compared with the Hg-air data. Figures 7-8 show a comparison between mercury injection and centrifuge water-oil Pc curves for 8 samples. The Hg-air Pc curves are converted to water-oil using  $\sigma \cos(\theta)$  of 367 and 23 mN/m for Hg-air and water-oil, respectively. Note that contact angle in this study refers to an effective contact angle for the respective saturation direction (Dumore and Schols 1974).

For the samples shown in Figure 7, there is a very good match between the mercury injection and centrifuge primary drainage capillary pressure curves even for dual porosity rocks. This confirms that proper design and interpretation of centrifuge experiment can capture the impact of dual porosity on capillary pressure curves, and equation (1) can be used to convert mercury injection Pc to equivalent oil water Pc in primary drainage.

However, for samples shown in Figure 8, there is clear discrepancy between the mercury injection and centrifuge Pc curves. The centrifuge water-oil curves were always lower than the corresponding mercury injection curves except when approaching low saturations. As shown in the figures, in some cases the water-oil Pc curve has the same shape as the mercury injection curve while for other samples the two curves have different shapes and the difference between them increases as the wetting phase saturation decreases.

### Effect of Core Cleaning on Drainage Pc

To investigate the cause of the difference between mercury injection and oil-brine centrifuge Pc curves, we considered the possible factors mentioned above, i.e., rock fluid interaction as a function of pore size, different fluid pairs, different samples used in the measurements or wettability effects due to ineffective cleaning.

The fact that a very good agreement between mercury injection and water-oil drainage Pc curve was obtained for some of the samples rules out the wettability effect due to aging by the crude oil, as aging only occurs after the oil has entered the pores. The pores that are not yet accessed by the crude oil remain water-wet hence the entry pressure for those pores will not be affected by using crude oil in the experiment, see Masalmeh (2002a & b).

The Pc discrepancies shown in Figure 8 can be explained by contact angle/wettability effect due to ineffective and incomplete cleaning (Masalmeh and Jing 2004, 2006). The cleaning method used at the early phase of the study (referred to as cleaning method (1) in the rest of the paper) is as follows: the plugs were cleaned by hot Soxhlett extraction using toluene followed by azeotropic mixture (84 vol% chloroform, 14.2 vol% methanol and 1.8 vol% water). Usually the toluene extraction continues for 2-3 weeks or more until the effluent becomes transparent. Then the azeotropic mixture is used for another 2-3 weeks or longer until the effluent becomes transparent again. Figures 7-8 show that for some samples not all the pores have been thoroughly cleaned to restore water-wet conditions e.g., cleaning may be less effective for smaller pores due to solvent accessibility and slowness in the diffusion process. The data also shows that ineffective cleaning has two effects on the Pc curves: it changes the shape of the curve (due to different  $\cos(\theta)$ ) and it shifts the Pc curve to the right (higher Sw) due to water trapping (Masalmeh 2001 and 2002a). Therefore, the difference between the water-oil capillary pressure and the mercury injection data can be used to check the efficiency of the cleaning method for the different pores. As a result of ineffective cleaning, using the primary drainage Pc from experiments involving water/oil to initialize the static model may lead to significant difference in initial oil in place and its distribution. Mercury-air derived drainage Pc curves should be used for the primary drainage process to establish the initial Sw distributions as ineffective cleaning of core samples does not appear to affect the mercury-air drainage Pc curves.

Since cleaning was found to be the reason for the mismatch between the water-oil and mercury injection data, another cleaning method was investigated which is referred to as cleaning method (2) (hot Soxhlett extraction followed by flow-through cleaning): The plugs were first cleaned using the above cleaning method (1) and then mounted in a Hassler core holder at a confining pressure of 30 bars. The plugs were alternately flooded with 100% chloroform at a back pressure of 5 bars. After flooding with about three pore volumes of chloroform the core was left to soak overnight. The procedure was repeated again with the next chloroform flood. In total more than 15 pore volumes of chloroform were used until the effluent became colourless. To further improve the effectiveness of cleaning, our current procedure for this reservoir rock/fluid system is to use flow-through cleaning method (2) mentioned above by alternating with different solvents (Chloroform, THF, Methanol).

The efficiency of the new cleaning method has been investigated. Three samples that showed the most difference between water-oil and mercury injection converted data were selected to go through cleaning method (2) and the water-oil drainage Pc curve was measured using the centrifuge. Figure 9 compares the new water-oil Pc curve measured on one of the samples with the mercury injection data. The figure shows an excellent match demonstrating that the new cleaning method is sufficient to achieve uniformly water-wet samples.

The centrifuge technique has also been used to measure the water-air Pc curves on a set of samples. The objective of this part is to confirm whether cleaning was the reason for the discrepancy between the water-oil and Hg-air data. The water-air data does not suffer from cleaning problems as air is the clear non-wetting phase. Figure 10 shows a comparison of Hg-air and centrifuge water-air Pc curves indicating a close match. The Hg-air Pc curves were converted to water-air using IFT of 480 mN/m for Hg-air and 72 mN/m for water-air, and the same contact angles for both fluid pairs were used. This finding differs from the commonly used literature values where contact angle of 140 is suggested for Hg-air and 0 for water-gas (Archer and Wall 1986).

### Imbibition Capillary Pressure Measurements

Imbibition Pc curves were measured on more than 40 samples from this reservoir. No spontaneous imbibition of water was observed on all the samples following aging with crude oil and connate water at reservoir temperature. As discussed in the previous section some of the plugs were cleaned by method (1) and as a result the water-oil primary drainage Pc curves were affected. Since the plugs did not start from strongly water-wet conditions during primary drainage (see previous section), it raised a question concerning the effect of this ineffective cleaning on the imbibition Pc curves. Could the wetting state after aging be significantly affected thus resulting in a more oil-wet rock? We know from experience that aging the sample for longer time (longer than 4-6 weeks) does not result in a stronger oil-wet system for carbonate reservoirs. Therefore, starting at a weakly water-wet condition may not result in a more strongly oil-wet system if no external factors are involved other than the adsorption of organic matter from the crude.

To verify the impact of ineffective cleaning on imbibition Pc curves, we have studied the imbibition Pc curves to see if any correlation between the negative Pc curves and the inefficient cleaning could be found. No such correlation was found, as higher contact angle during primary drainage did not correlate with higher contact angle during imbibition. In addition, imbibition capillary pressure curves were repeated on the samples that had gone through the further cleaning method (2). Figure 11 shows the imbibition Pc after the cleaning methods (1) and (2). The data show no difference between the two sets of imbibition Pc curves (one following the ineffective cleaning method 1 and the other following the thorough cleaning procedure 2).

Figure 12 shows the imbibition capillary pressure curves measured on 31 samples. Similar to drainage, the data are measured on samples from different permeability and porosity classes and different rock textures. For all the samples the imbibition experiment started from the average water saturation at the end of the primary drainage centrifuge. This average saturation is usually higher than connate water and the difference with connate water increases for samples which were not effectively cleaned. Therefore the spread in the starting points (at zero Pc) does not reflect a spread in connate

water saturations. The imbibition Pc curves in general follow the same classification scheme as for the drainage Pc curves. Group A has low entry pressure and starts to increase smoothly, the residual oil saturation varies between 5-15%. Group B has also low entry pressure (though higher than group A) and then the Pc increases faster as the water saturation increases. The residual oil saturation varies between 8%-16%. Group C has a high entry pressure (2-4 Psi), and the residual oil saturation varies between 5-18%. Similar to connate water, there is in general a trend of increasing residual oil saturation as porosity decreases within each group. However, there is no correlation of  $S_{or}$  with porosity across the groups.

### Deriving Imbibition Pc from Drainage Pc

As no spontaneous imbibition was observed for this type of oil-wet carbonate reservoir, the water displacing oil process during imbibition followed the same pore-filling sequence as in the primary drainage experiment, i.e., non-wetting phase enters the largest pores first. Therefore, based on a conceptual pore-space model for the oil-wetting system, imbibition and drainage should show a mirror image of each other if the contact angle hysteresis and oil trapping function are accounted for. The imbibition Pc can be derived from the measured drainage Pc (after conversion to oil/water reservoir conditions) in the following steps:

1. Multiplying the drainage Pc by the ratio of the contact angles (imbibition vs. drainage). IFT terms cancel out since we refer to the same fluid pair:

$$P_c^{imb} (S_w^{imb}) = P_c^{dra} (S_w^{dra}) * \frac{\cos(\theta_{imb})}{\cos(\theta_{dra})} \quad (2)$$

2. Imbibition experiment starts at  $S_w = S_{wc}$ , water saturation of the imbibition Pc is then given as:

$$S_w^{imb} = 1 - S_w^{dra} + S_{wc} \quad (3)$$

3. During imbibition oil trapping takes place and the amount of this trapping is a function of the initial oil saturation. The trapped oil saturation ( $S_{otrap}$ ) can be derived either experimentally or from correlations. In this study we used a linear correlation:

$$S_{otrap} (S_o) = S_{otrap}^{max} * \left( \frac{1 - S_w^{dra}}{1 - S_{wc}} \right) \quad (4)$$

$$S_{otrap}^{max} = S_{orw}; \quad S_{otrap}^{min} = 0$$

where  $S_{orw}$  is the maximum waterflood  $S_{or}$  measured at the end of imbibition.

4. The water saturation during imbibition is calculated from drainage as:

$$[S_w]^{imb} = [1 - S_w^{dra} + S_{wc} - S_{otrap} (S_o)] \quad (5)$$

5. The final step in the conversion is to substitute equation 5 in equation 2, the imbibition Pc curve can be derived from drainage Pc as follows:

$$P_c^{imb} (S_w^{imb}) = P_c^{dra} (1 - S_w^{dra} + S_{wc} - S_{otrap}) * \frac{\cos(\theta_{imb})}{\cos(\theta_{dra})} \quad (6)$$

where  $\theta_{dra}$  and  $\theta_{imb}$  are the contact angles in drainage and imbibition, respectively.

In order to calculate the imbibition Pc curves as shown above, it is necessary to have calibration on the contact angle hysteresis and oil trapping function in the waterflood imbibition process. Both can be obtained from a limited number of SCAL measurements on representative core materials taken from the same reservoir.

For this carbonate reservoir under investigation, the samples with uni-modal pore size distributions showed a consistent contact angle range of 108-111 degrees as shown in Masalmeh and Jing (2006). Whereas for samples with bi-modal pore systems, the imbibition Pc curve could not be converted to the drainage Pc curve using a constant contact angle as the large pores showed higher contact angles ( $\sim 120 \pm 2$  degrees) than the small pores ( $\sim 100 \pm 3$  degrees). This appears to indicate that the large pore system became more oil-wet than the small pore system for the samples with bi-modal pore size distribution. Further research is needed to fully understand the underlying reasons for the observed contact angle distribution in carbonates.

Figure 13 shows the calculated and measured imbibition Pc curves indicating an excellent agreement. With more imbibition Pc data becoming available and covering a wider range of carbonate reservoirs, it may become possible to further verify the imbibition contact angle distributions shown above as a function of reservoir rock and fluid properties and build an analogue database for reservoir applications in the absence of SCAL measurements. It's important to note the above procedure for deriving imbibition Pc from the corresponding drainage curves only apply to oil-wet and mixed-wet carbonate reservoirs that show no spontaneous imbibition of water in imbibition Pc curves. This seems to be generally the case for limestone oil reservoirs in the Middle East.

### Capillary Pressure Model: Drainage and Imbibition Pc Curves

In this section, we will present a set of analytical equations that can be used to match Pc curves measured on all the samples (both uni-modal and multi-modal pore size distributions) used in this study.

The measured drainage (Pcd) and imbibition (Pci) capillary pressure curves can be fitted using the following equations:

$$P_c^{dra} = \frac{C_{wd}}{\left[ \frac{S_w - S_{wc}}{1 - S_{wc} - S_{or}} \right]^{a_{nd}}} + \frac{C_{od}}{\left[ \frac{1 - S_w - S_{or}}{1 - S_{wc} - S_{or}} \right]^{a_{od}}} + b_d (S_{w-c}^{dra} - S_w) \quad (7)$$

$$P_c^{imb} = \frac{c_{wi}}{\left[ \frac{S_w - S_{wc}}{1 - S_{wc} - S_{or}} \right]^{a_{wi}}} + \frac{c_{oi}}{\left[ \frac{1 - S_w - S_{or}}{1 - S_{wc} - S_{or}} \right]^{a_{oi}}} + b_i(S_{w_c}^{imb} - S_w) \quad (8)$$

where in drainage  $b_d$  is zero for water saturation higher than critical saturation value  $S_{w_c}^{dra}$ , in imbibition  $b_i$  is zero for water saturation less than  $S_{w_c}^{imb}$  and  $c_{wd}$ ,  $c_{od}$ ,  $a_{wd}$ ,  $a_{od}$ ,  $b_d$ ,  $c_{wi}$ ,  $c_{oi}$ ,  $a_{wi}$ ,  $a_{oi}$  and  $b_i$  are fitting parameters used to fit experimental data. For primary drainage, the  $S_{or}$  term in equation (7) becomes zero. The formulae are an extension from Masalmeh et al. (2007). The first and second terms are modified from Brooks and Corey (1966) and Skjaeveland et al. (1998), respectively. We introduce the third term in the equations to describe different shapes of capillary pressure curves (e.g., for bi-modal pore size distributions) as the first two terms alone could not match the experimental data particularly for samples of dual porosity or samples of a wide range of pore size distributions. Figure 14 shows both measured and model generated Pc curves for three samples of different pore size distribution. The Pc curves shown in Figure 14a can be generated assigning zero value for  $b_d$  and  $b_i$ , however, the curves shown in Figure 14b-c can only be generated with the third term included. This is found to be the case for all heterogeneous bi-modal samples and for samples of wide pore size distributions. Masalmeh et al. (2007) also extended this capillary pressure model for heterogeneous carbonates to cover water/oil capillary transition zones involving bounding and scanning curves.

### Impact on Waterflood Remaining Oil Saturation Predictions

**Simulation model description:** Mechanistic sector models were constructed to evaluate the impact of the reservoir characterisation and modelling workflow procedure discussed in this paper on remaining oil saturation distribution. The waterflood simulations were performed using both 2D and 3D dynamic models based on detailed geological modelling and petrophysical characterisation. For simplicity and illustration purpose, in this section we present results using a 2D (50x160) element model of 160 layers with 30 cm vertical resolution and the grid size in the x direction is 20 m. Porosity and permeability within each layer is set to be constant. Permeability and porosity distributions as a function of depth are similar to that shown in Figure 2. In all the simulations carried out in this work, a vertical injector was placed at one end of the model and a producer was placed at the other end. Initial fluid distributions were assigned to the model using drainage capillary pressure curves and then imbibition capillary pressure is used as waterflood starts. The capillary pressure hysteresis model in MoReS (Shell in-house simulator) is utilised. The use of drainage and imbibition capillary pressure curves for both model initialisation and dynamic simulation was discussed by Masalmeh et al. (2007).

**Impact of Capillary Pressure Models:** The impact of

different capillary pressure models on oil recovery and remaining oil saturation distribution is evaluated by comparing three different Pc models: (1) Pc\_model1: drainage capillary pressure used for both initialisation and waterflooding; (2) Pc\_model2: drainage capillary pressure used for initialisation; then, zero capillary pressure used once waterflooding starts; (3) Pc\_model3: correct implementation of the capillary pressure model (Eqs. 10 -11) with both drainage and imbibition anchored to SCAL measurements, including bounding and scanning curves.

Saturation logs have been generated at a distance of 200 m from the injector as a function of pore volume injected for the three capillary pressure models. Figure 15 shows the simulated saturation logs of the runs using Pc\_model2 and Pc\_model3. The data shows that capillary pressure modelling has a significant impact on remaining oil saturation distribution. This point was discussed in detail in Masalmeh et al. (2003 and 2007), where it was shown that for mixed-/oil-wet heterogeneous reservoirs, imbibition capillary pressure is one of the most important parameters that affects waterflooding performance and sweep efficiency. It can behave as a capillary barrier, preventing crossflow between the different layers and resulting in poor sweep efficiency. Preserving both low- and high-permeability layers, as well as their capillarity contrasts, in the reservoir model has a significant impact on the reservoir-performance predictions because it controls gravity/capillary crossflow and channelling of injected water. Production performance and recovery will differ for various input assumptions of wettability, shapes of saturation functions, and vertical permeability profiles. The same simulation results as in the case of Pc\_model2 (i.e., zero imbibition Pc) were obtained when the same imbibition Pc curve was applied to all the rock types in the model. This further indicates the critical importance of preserving the correct imbibition Pc contrasts between different rock types for modelling waterflood performance and remaining oil saturation distribution for this type of oil-wet carbonates.

It is important to map the fluid distribution in the reservoir under waterflood for the different scenarios discussed because the remaining oil distribution will significantly impact any future improved-oil-recovery (IOR) or enhanced-oil-recovery (EOR) options. For example, to answer the question of whether we should target the remaining oil saturation either by infill drilling or by an EOR process, it is necessary to know accurately the remaining oil distribution due to waterflooding.

### Conclusions

This paper presents an improved reservoir characterisation and modelling procedure for heterogeneous carbonate reservoirs with a focus on dynamic reservoir properties. The results and conclusion are drawn based on a detailed and comprehensive special core analysis study carried out on rock samples selected from a heterogeneous carbonate reservoir, combined with detailed mechanistic dynamic simulation integrating static and dynamic behaviours. The main conclusions and findings are summarised as follows.

1. The primary drainage Pc curves measured using two

different methods (mercury injection vs. centrifuge oil-brine) have been compared for the same plugs from different porosity and permeability ranges. Close agreement between the Pc curves has been observed if the core samples are thoroughly cleaned and made uniformly water-wet.

2. Water-oil primary drainage Pc curves can be significantly affected by ineffective core cleaning which, if not properly recognized and reconciled against Hg-air Pc curves, can have severe impact on STOIP calculations especially for the low permeability reservoirs. In general, Hg-air capillary pressure (with the appropriate conversion to reservoir rock/fluid systems) should be used for the primary drainage to establish the initial water saturation distributions in carbonate reservoirs.
3. Despite the significant impact of cleaning on primary drainage water-oil Pc curves, ineffective cleaning seems to have little or no impact on imbibition Pc curves if no external factors other than crude oil contributed to wettability alteration.
4. We propose a procedure to relate imbibition capillary pressure with primary drainage for both uni-modal and bi-modal pore size distributions taking into account the effect of wettability in carbonates. Based on certain SCAL experiments, it's possible to generate the contact angle distributions for imbibition and oil trapping behaviour, and then convert the primary drainage Pc curves to imbibition Pc curves taking into account the effect of wettability.
5. We present an improved capillary pressure model for both drainage and imbibition cycles to capture the complexity of the carbonate pore structure for different wetting systems. This model can be calibrated by SCAL measurements and allows drainage and imbibition Pc implementation in reservoir simulations on a rock type basis.
6. We show that the waterflood remaining oil saturation depends crucially on capturing the detailed reservoir geology at the appropriate scales and the correct input of dynamic rock properties, in particular, the correct imbibition capillary pressure curves for heterogeneous carbonate reservoirs. This has profound implications on the choice and optimum design of any subsequent EOR processes.

## Nomenclature

FWL	= free water level
$a_{od}, a_{oi}, a_{wd}, a_{wi}, b_d, b_i, c_{od}, c_{oi}, c_{wd}, c_{wi}$	= fitting parameters in capillary pressure model
$P_c$	= drainage capillary pressure [=] F/L <sup>2</sup>
$S_{otrap}$	= trapped oil saturation
$S_{or}$	= residual oil saturation
$S_{wc}$	= connate water saturation
$S_{w-c}$	= water saturation variable in equations 7-8

## Subscripts

o	= oil
w	= water
d	= drainage
i	= imbibition
r	= residual
R	= Reservoir
L	= Laboratory

## Superscripts

dra	= drainage
imb	= imbibition
max	= maximum

## Greek Letters

$\theta$	= contact angle
$\sigma$	= interfacial tension

## Acknowledgements

We thank our colleagues in Shell Technology Oman and the Shell Carbonate Development Team for stimulating discussions. We thank Sjaam Oedai for the experimental SCAL measurements.

## References

- Archer, J.S. and Wall, C.G.: *Petroleum Engineering Principles and Practice*, Graham & Trotman, (1986).
- Brooks, R.H. and Corey, A.T.: "Properties of Porous Media Affecting Fluid Flow", J. of the Irrigation and Drainage Division, Proc. of ASCE, 92, No. IR2, (1966) 61-88.
- Giot D., Dawans J.M., King, R. and Lehmann, P.: "Tracking Permeability in Major Limestone Reservoir: From Rock Observation to 3D Modelling", SPE 87233, 9th ADIPEC, Abu Dhabi, Oct. 15-18, 2000
- Dunham, R.J., 1962. Classification of carbonate rocks according to depositional textures. In: Ham, W.E. (ed.) Classification of carbonate rocks. Memoir American Association of Petroleum Geologists, 1, 108-121.
- Dumore, J.M. and Schols, R.S.: "Drainage Capillary Pressure Functions and the Influence of Connate Water", SPEJ (1974) 437-444.
- Forbes, P.: "Centrifuge Data Analysis Techniques: An SCA Survey on The Calculation of Drainage Capillary Pressure Curves from Centrifuge Measurements", SCA 9714 presented at the SCA 1997 conference, Calgary, Canada (1997).
- Harrison, R. and Jing, X.D. "Saturation Height Methods and Their Impact on Volumetric Hydrocarbon in Place Estimates", SPE 71326, SPE Annual Technical Conference and Exhibition, New Orleans, Louisiana, 30 September–3 October (2001).
- Hamon, G.: "Two -Phase Flow Rock-Typing: Another Perspective", SPE 84035, SPE Annual Technical Conference and Exhibition, Denver, Colorado, Oct 5-8, (2003).
- Hassler, G.L. and Brunner, E.: "Measurement of Capillary

- Pressure in Small Core Samples”, Trans. AIME (1945), Vol 160.
- Honarpour, M.M., Djabbarah, N.F. and Kralik, J.G.: “Expert-Based Methodology for Primary Drainage Capillary Pressure Measurements and Modelling”, SPE 88709 presented at the ADIPEC conference, Abu Dhabi, (2004).
- Jennings, J.W. and Lucia, F.J.: “Predicting Permeability from Well Logs on Carbonates with a Link to Geology for Interwell Permeability Mapping”, SPE 84942, SPE Reservoir Evaluation & Engineering, p.215-225, August, (2003).
- Leal, L., Barbato, R., Quaglia, A., Porrai, J.C. and Lazarde, H.: “Bimodal Behaviour of Mercury-Injection Capillary Pressure Curve and Its Relationship to Pore Geometry, Rock-Quality and Production Performance in Laminated and Heterogeneous Reservoirs”, SPE 69457, SPE Latin America and Caribbean Petroleum Engineering Conference, Buenos Aires, March 25-28, (2001).
- Lucia, F.J.: *Carbonate Reservoir Characterization*, Springer-Verlag, Berlin (1999).
- Maas, J.G. and Schulte A.M.: “Computer Simulation of Special Core Analysis (SCAL) Flow Experiments Shared on the Internet”, SCA-9719 presented at the SCA 1997 conference, Calgary, Canada (1997).
- Marzouk, I., Takezaki, H and Suzuki, M.: “New Classification of Carbonate Rocks for Reservoir Characterization”, SPE 49475, 9th ADIPEC, Abu Dhabi, Oct. 15-18, (2000).
- Masalmeh, S.K.: “Experimental Measurements of Capillary Pressure and Relative Permeability Hysteresis” SCA 2001-23 presented at the SCA 2001 conference, Edinburgh, September (2001).
- Masalmeh S.K.: “Studying the Effect of Wettability Heterogeneity on the Capillary Pressure Curves Using the Centrifuge Technique”, Journal of Petroleum Science and Engineering, 33 (2002a) 29-38.
- Masalmeh, S.K.: “The Effect of Wettability on Saturation Functions and Impact on Carbonate Reservoirs in the Middle East “, SPE 78515, 10th ADIPEC, Abu Dhabi, Oct. 13-16, (2002b).
- Masalmeh, S.K., Jing, X.D., van Vark, W., van der Weerd, H. Christiansen, S. and van Dorp, J.: “Impact of SCAL on Carbonate Reservoirs: How Capillary Forces Can Affect Field Performance Predictions” SCA 2003-36 presented at the SCA 2003 conference, Pau, France, October (2003).
- Masalmeh, S.K., Jing, X.D.: “Carbonate SCAL: Characterization of Carbonate Rock Types for Determination of Saturation Functions and Residual Oil Saturation”, SCA-08 presented at the SCA 2004 conference, Abu Dhabi, October (2004).
- Masalmeh, S.K. and Jing, X.D. “Capillary Pressure Characteristics of Carbonate Reservoirs: Relationship between Drainage and Imbibition Curves”, SCA 2006-16, Reviewed Proc. International Symposium of the Society of Core Analysts, Trondheim, Norway, 12-16 September, (2006).
- Masalmeh, S.K., Abu Shiekah, I. and Jing, X.D.: “Improved Characterization and Modeling of Capillary Transition Zones in Carbonate Reservoirs”, SPE paper 109094, SPE Reservoir Evaluation & Engineering, Vol. 10 (2): 191-204 APR (2007).
- Moctezuma, A., Békri, S. Laroche, C. and Vizika O. "A Dual Network Model for Relative Permeability of bimodal rocks: Application in a Vuggy Carbonate", SCA 2003-12, Pau, France, Sep. 22-25, 2003.
- Morrow, N.R. and Melrose, J.C.: “Application of Capillary Pressure Measurements to the Determination of Connate Water Saturation”, *Interfacial Phenomena in Petroleum Recovery*, N.R. Morrow (ed.), Marcel Dekker, New York City (1991) 257-287.
- O’Meara, D.J., Hirasaki, G.J. and Rohan, J.A.: “Centrifuge Measurements of Capillary Pressure: Part 1-Outflow Boundary Conditions”, SPE 18296, (1992).
- Porrai, J.C. and Campos, O.: “Rock Typing: A key Approach for Petrophysical Characterization and Definition of Flow Units, Santa Barbara Field, Eastern Venezuela Basin”, SPE 69458, SPE Latin America and Caribbean Petroleum Engineering Conference, Buenos Aires, March 25-28, 2001.
- Ramakrishnan, T.S., Rabaute, A. Fordham, E.J., Ramamoorthy, R., Herron, M., Matteson, A. and Raghuraman, B.: “A petrophysical and Petrographic Study of Carbonate Cores from the Thamama Formation”, SPE 49502, 9th ADIPEC, Abu Dhabi, Oct. 15-18, 2000.
- Sallier, B. and Hamon, G.: “Micritic Limestones of the Middle East: Influence of Wettability, Pore Network and Experimental Techniques on Drainage Capillary Pressure”, SCA2005-08 presented at the SCA 2005 conference, Waterloo, Canada, (2005).
- Skjaeveland, S.M., Siqveland, L.M., Kjosavik, A., Hammervold, W.L., Virnovsky, G.A.: “Capillary Pressure Correlation for Mixed-Wet Reservoirs”, SPE 39497, paper presented at the SPE India Oil and Gas Conference and Exhibition, New Delhi, India, February 17-19, (1998).
- Silva, F.P.T., Ghani, A., Al Mansouri, A. and Bahar, A.: “Rock Type Constrained 3D Reservoir Characterization and Modelling”, SPE 78504, 10th ADIPEC, Abu Dhabi, Oct. 13-16, 2002.
- Valvatne, P.H., Jing X.D. and Smits, R.M.M. “Predicting Pore Geometric and Wettability Effects on Relative Permeability Using Pore-Scale Network Modelling”, SCA 2004-26, Reviewed Proc. International Symposium of the Society of Core Analysts, Abu Dhabi, October, (2004).

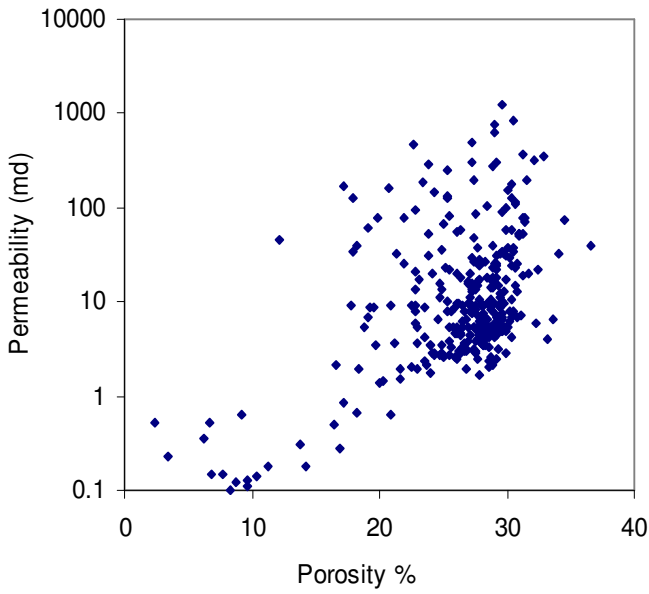


Figure 1: Porosity vs Permeability of the sample set used in the study

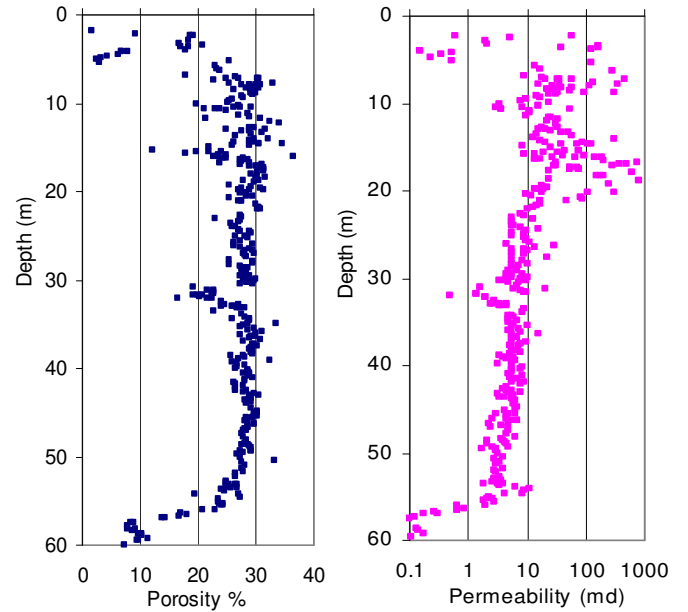


Figure 2: Porosity and permeability as a function of normalized depth

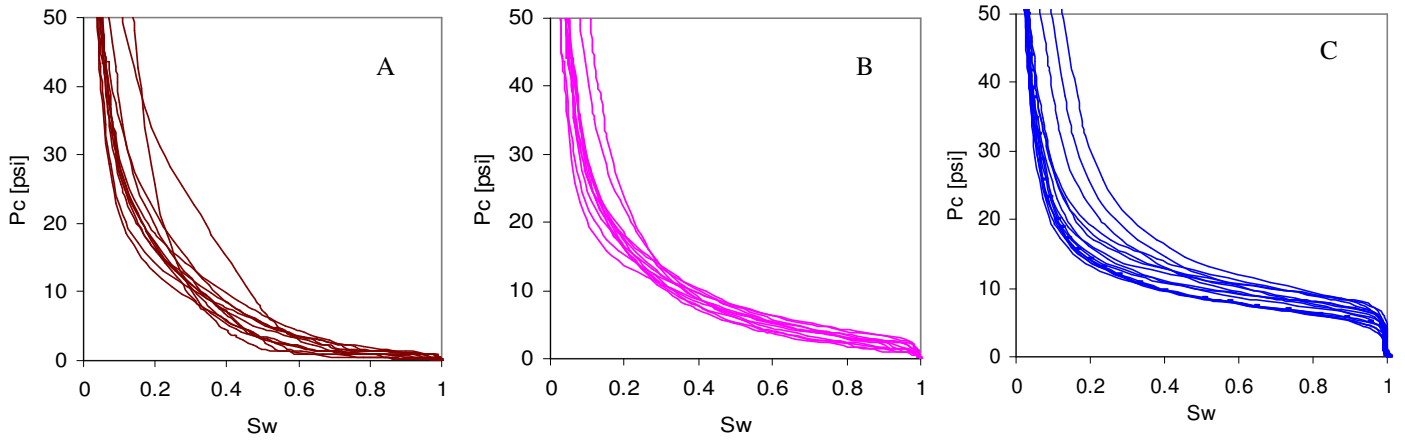


Figure 3: Drainage capillary pressure curves - examples illustrating the three different groups (A, B and C)

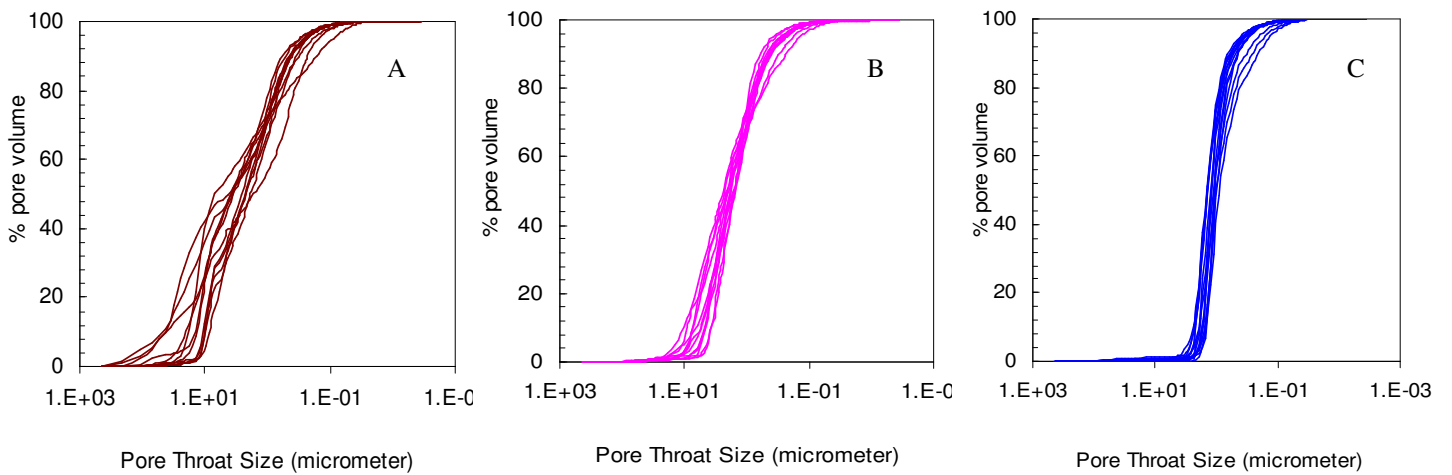


Figure 4: Pore throat size distributions for the three different groups (A, B and C) shown in Figure 3.

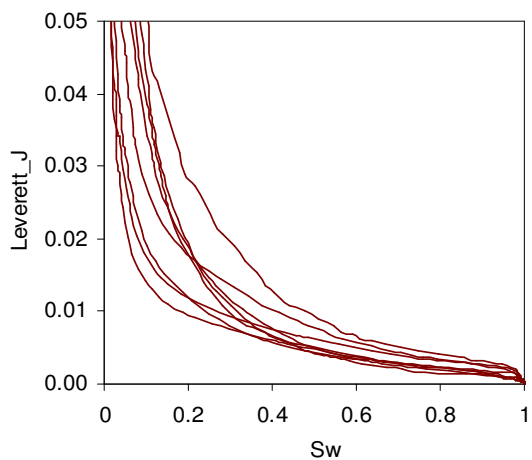


Figure 5: Leverett J-Function for samples from group B.

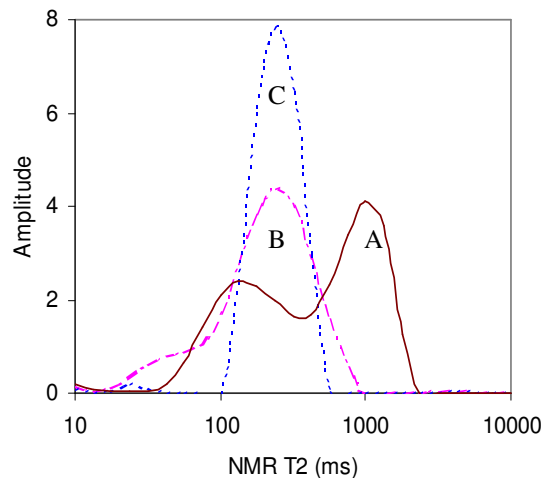


Figure 6: Example NMR T2 distributions representing each of the three group (A, B and C).

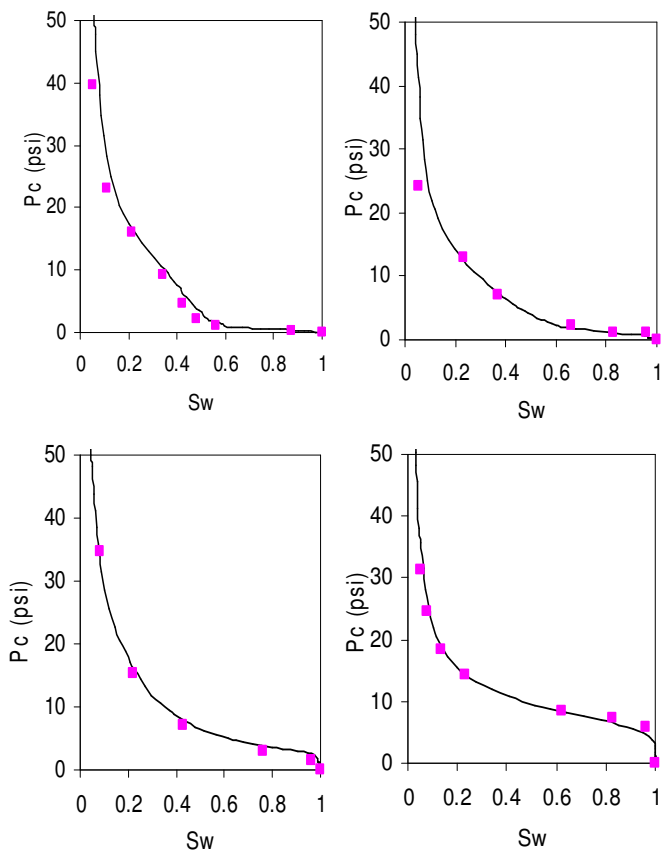


Figure 7: Comparing centrifuge oil-water Pc (symbols) to Hg-air Pc (lines) curves for 4 samples - a close match is obtained for this group of samples.

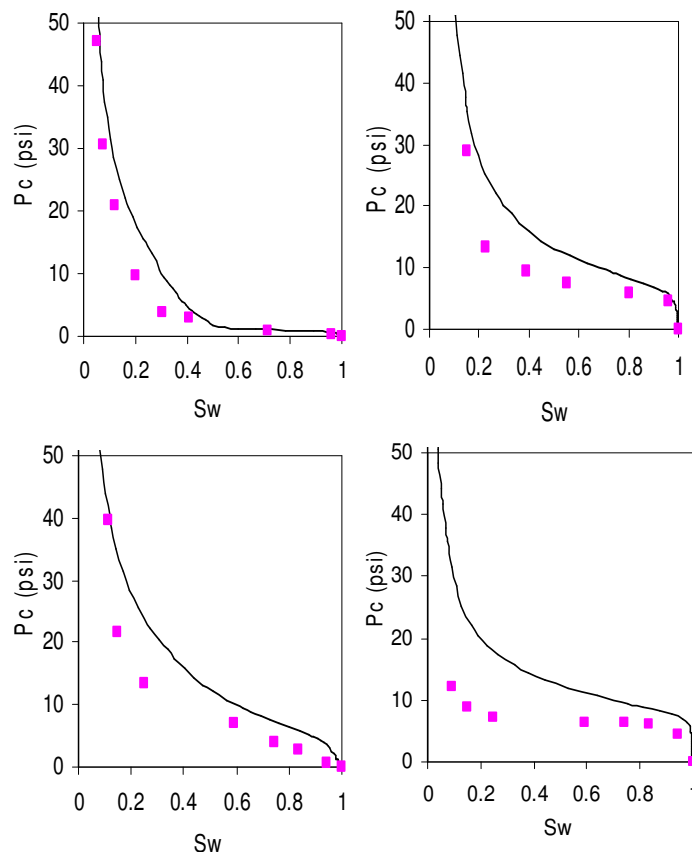


Figure 8: Comparing centrifuge oil-water Pc (symbols) to Hg-air Pc (lines) curves for 4 samples - no match is obtained for this group of samples due to inefficient cleaning.

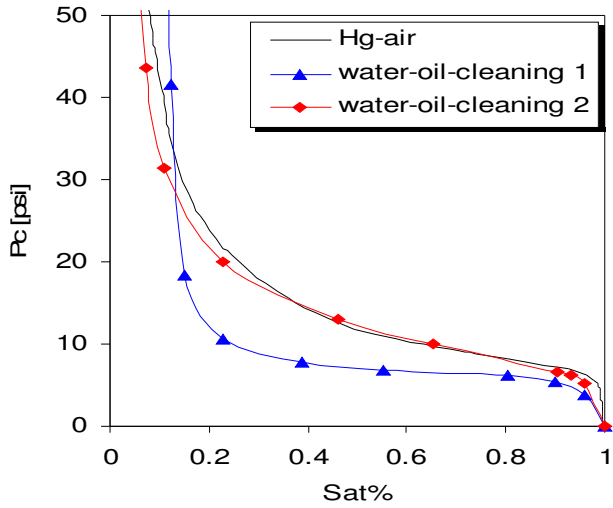


Figure 9: Drainage Pc curves measured on one of the samples following two different cleaning methods (compared against the Hg-air derived curve).

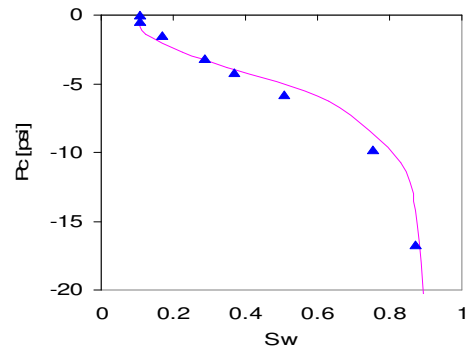


Figure 11: Imbibition Pc measured on the same sample (symbols = imbibition after clean (1); line = imbibition after clean (2)).

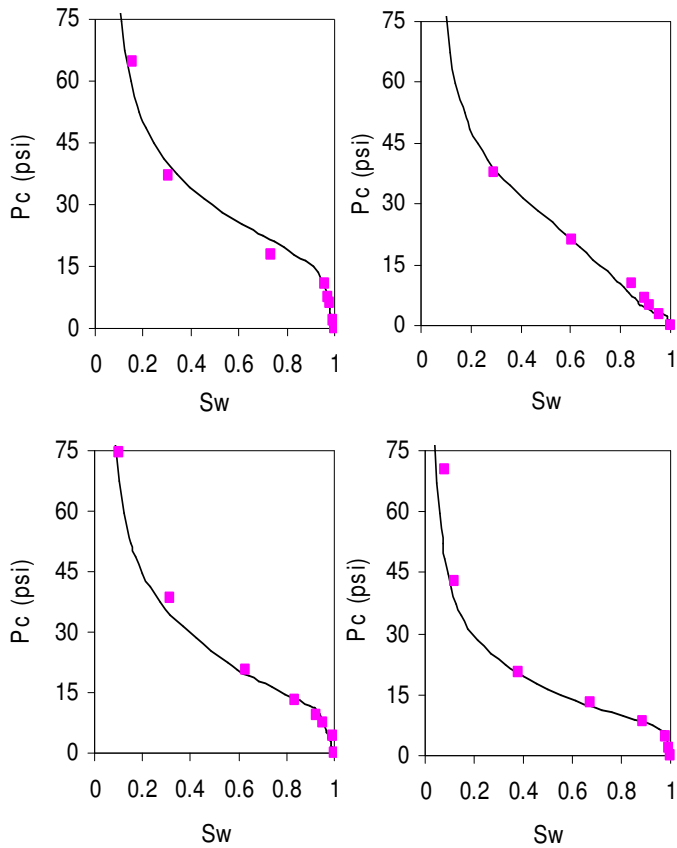


Figure 10: Comparing centrifuge water-air Pc (symbols) to Hg-air Pc (lines) curves for 4 samples, a close match is obtained.

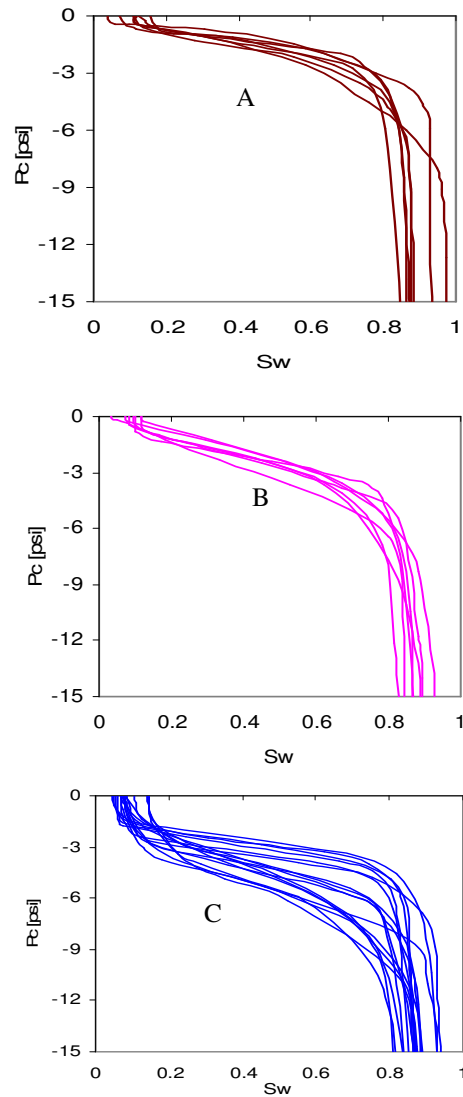


Figure 12: Imbibition Pc curves measured on 31 samples representing the three groups (A, B, C) shown in Figs 3-4.

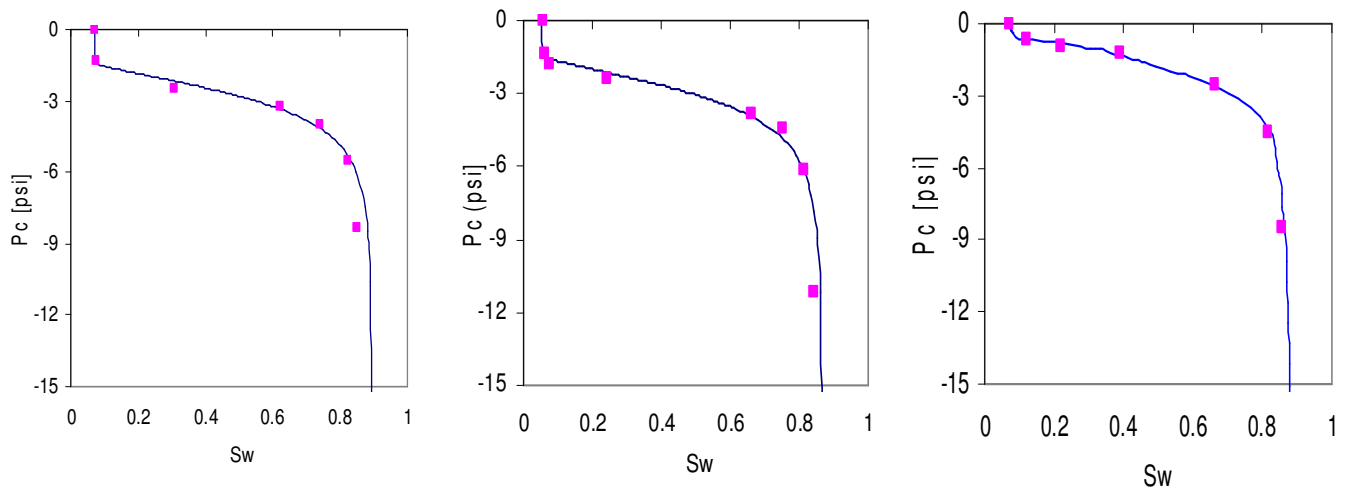


Figure 13: Comparison of measured (symbols line) and calculated (solid lines) imbibition Pc curves.

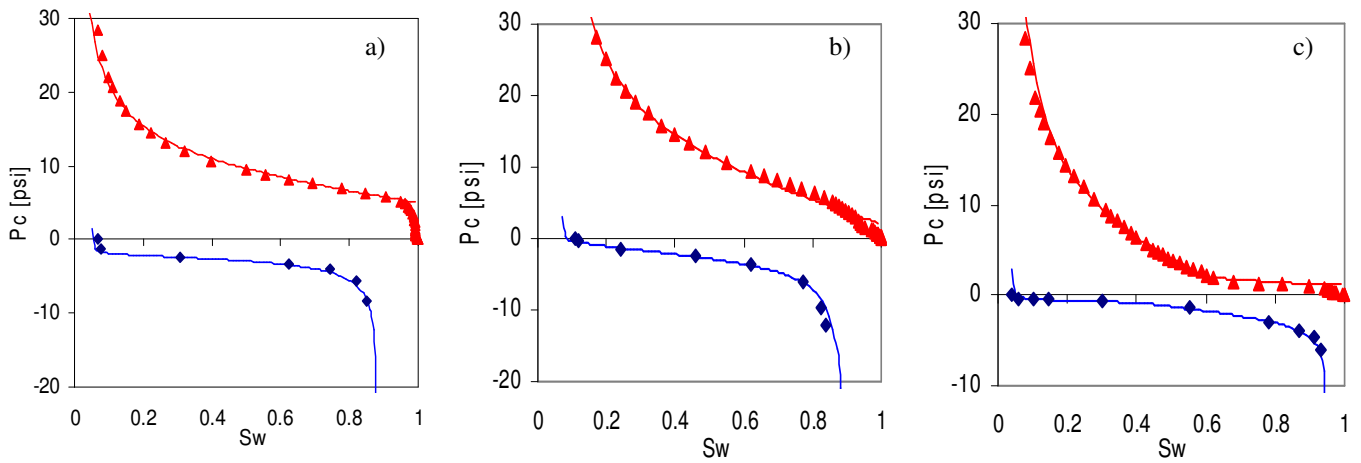


Figure 14: Model (lines) and measured (symbols) Pc bounding curves of a) low permeability sample of uniform pore size distribution, b) low permeability sample of wide range of pore size distribution and c) high permeability sample of dual porosity system.

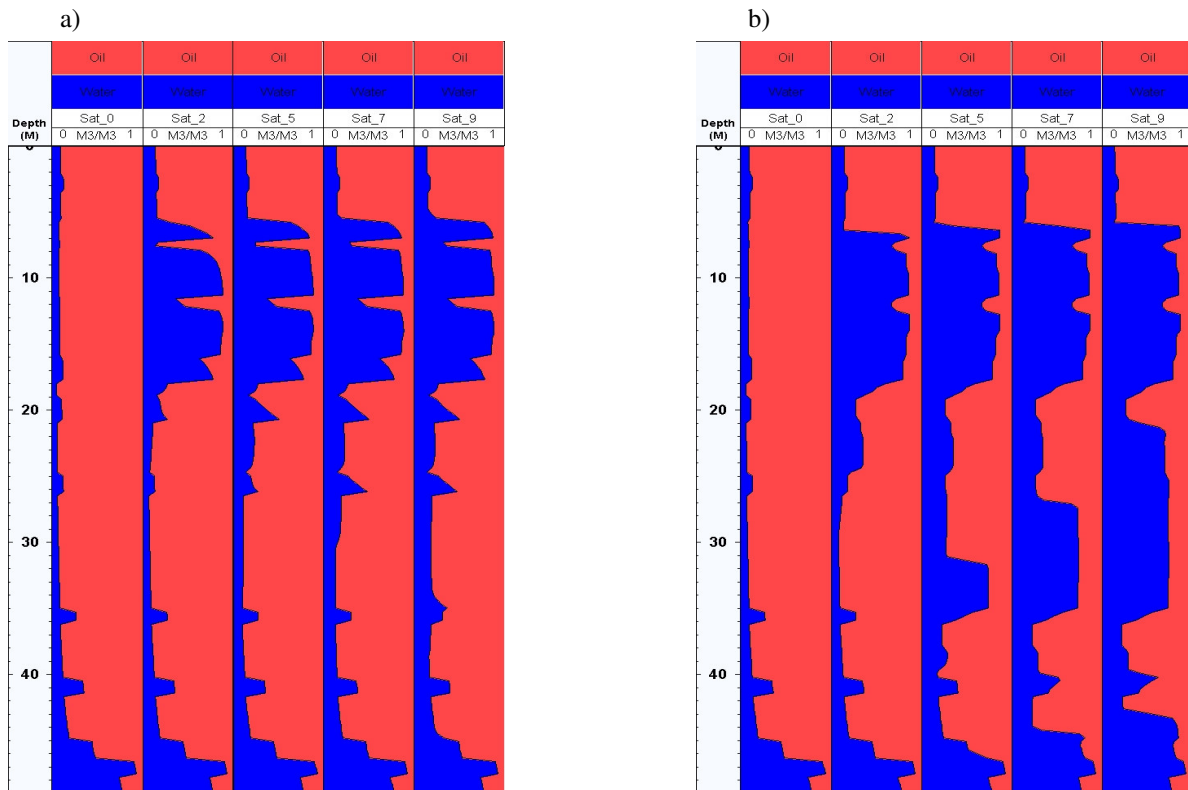


Figure 15: Saturation logs for an observation well 200 m away from the injector at 0, 0.2, 0.5, 0.7 and 0.9 PV of water injection - generated using a 2D sector model: a) Correct Pc model with rock-type dependency was implemented using measured drainage and imbibition Pc curves, b) The same imbibition Pc (or zero imbibition Pc) for all rock types was used to model water flooding. Blue = water; Red =oil.